Influence of the anisotropy of the material on the pore water pressures within the downstream shell of a rockfill dam in overtopping scenario

J.C. Díaz[1], M.A. Toledo[1] and R. Morán[1]

[1]*Technical University of Madrid (UPM), C/. Profesor de Aranguren S/N, 28040, Madrid, Spain*

Abstract

The compaction tasks developed during the construction of the shell of rockfill dams may crush the particles of the material close to each surface layer. If so, this can cause local variations in the permeability of the material and consequently an alteration of the hydraulic pattern of the seepage through the shell as well as the pore water pressures developed within it. This article summarizes the study of this effect through hydraulic numerical modelling developed by the FLOW-3D commercial code. Such study presents a discussion about the influence of the altered and unaltered zones of the layers on the general flow pattern, particularly in the downstream water level depths, hydraulic gradients and pore water pressures. The tests have been set up with a non-laminar seepage equation using a parabolic relation between hydraulic gradient and seepage velocity. The numerical models simulate homogeneous rockfill formed by isotropic layers with different permeability, which result in an overall anisotropic dam body.

1 Introduction

Overtopping is the main cause of embankment dam failure, including rockfill dams. This cause is above body and foundation internal erosion as well as earthquakes (Morán & Toledo, 2011). In the initial phase, overtopping can cause damage in downstream layers, due to material loss by dragging, erosion or mass sliding (Morán, 2014). Specifically, overtopping seepage in a highly permeable rockfill dam has been analyzed by conventional methods that consider the shell as a homogeneous and isotropic element where flow enters from the crest and descends vertically toward the foundation. The flow depth rises within the rockfill and flow exits through the downstream toe. The water circulation through coarse porous media, such as rockfill, gravel or even larger sands has the particularity of exhibiting a non-linear relationship between hydraulic gradient and seepage velocity (Toledo, et al., 2012). This behavior is limited to the through flow capacity of granular media (Toledo, 1997). When overtopping discharge exceeds this capacity, the skimming flow over the shoulder initiates. This approach excluded the anisotropy caused by the compaction of the lifts that changes the granulometry when particles on the surface are crushed. If the alteration degree is considerable, it can produce a variation between horizontal and vertical permeabilities. If this difference is significant, the media should be modeled as anisotropic (Toledo, 1997). Cruz analyzes the saturation line in a rockfill shell whose ratio between horizontal and vertical equivalent permeability is 22. In such case, the flow depth at the toe of the dam increases 50% compared to an isotropic case (Cruz, et al., 2010). The author concludes that a greater horizontal permeability related to the vertical has a negative effect on the rockfill stability when flow through occurs.

2 Theoretical basis and numerical model description

2.1 Forchherimer flow resistance model

The author characterizes energy losses within porous media as a combination of expressions with linear and quadratic terms (Flow Science, 2015):

$$-\nabla p = (a + b|u_{bulk}|)u_{bulk} \quad (1)$$

Where, ∇p is the pressure gradient in porous media, u is the apparent velocity, a and b are material coefficients which can be experimentally defined according to Ergun formulation according to a parabolic resistance equation

$$-i = a_e \cdot u_{bulk} + b_e \cdot {u_{bulk}}^2 \quad (2)$$

The equation (2) can be combined in an expression that starts from Darcy's linear resistance model which states that, flow velocity through a porous media is directly proportional to the pressure difference applied:

$$u_{bulk} = -\frac{K}{\mu}\nabla p \quad (3)$$

Where, K is intrinsic permeability of material, and μ is the water dynamic viscosity.

$$F_d u_{mic} = -\frac{1}{\rho}\nabla p = \frac{\mu}{p}\frac{1-\emptyset}{\emptyset}\left[A\frac{1-\emptyset}{\emptyset} + B\frac{Re_p}{d_{poro}}\right]u_{mic} \quad (4)$$

Where A and B are the linear and quadratic resistance coefficients that are used by the numerical code to adjust the seepage model, and ρ is the water density. Replacing in Equation (1) results in an expression that relates A and B for pressure losses per unit length as a function of the macroscopic velocity. A and B are related to the factors a and b, which can be obtained experimentally.

$$-\nabla p = A \cdot |u_{bulk}|\mu\frac{(1-\emptyset)^2}{\emptyset^3} + B \cdot |u_{bulk}|^2\rho\frac{(1-\emptyset)}{\emptyset^3} \quad (5)$$

$$A = a\frac{\emptyset^3}{\mu(1-\emptyset)^2}, \qquad B = b\frac{\emptyset^3}{\rho(1-\emptyset)} \quad (6)$$

If the porous media permeabilities are known, these values can be transformed through (7) in which $K1$ is the intrinsic permeability of material and $K2$ is the inertial permeability (Flow Science, 2015).

$$a = \frac{\mu}{K_1}, \qquad b = \frac{s\rho}{K_2} \quad (7)$$

Replacing (7) in equation (6) produces the following expression (8). If $K2$ is unknown the coefficient B will be set as 0 and the model is considered laminar according to Darcy equation.

$$A = \frac{\emptyset^3}{(1-\emptyset)^2 K_1}, \qquad B = \frac{\emptyset^3}{(1-\emptyset)K_2} \quad (8)$$

2.2 Mesh criteria

Flow-3D uses FAVOR algorithm, which defines mesh and geometry independently. It allows adding, moving or eliminating geometric elements without affecting configuration. The dimensions of each mesh block are defined in directions X_{min}, X_{max}, Y_{min}, Y_{max}, Z_{min}, Z_{max}; X corresponds to the longitudinal axis channel, considered positive in the direction of the flow, Y is transversal to the channel and vertical Z, positive upwards. A mesh block of X=9.0 m; Y=0.1 m and Z=1.6 m with a cell size of 0.02m is proposed, so as to get a better resolution. The ratio between dam and cell height (H_{dam}/H_{cell}) is 1/50.

Three mesh blocks were defined. Two of them, with cell size 0.02m, were overlapped in the approach zone on a solid that allows water inlet by the crest and the third, with cell size 0.01m, which is divided into thinner layers so as to have at least 4 cells along the thickness which allow enough precision in results. The ratio between altered layer thickness and cell size (H_{C3}/H_{cell}) is 1/4.

Figure 1. Mesh block of the calibration models

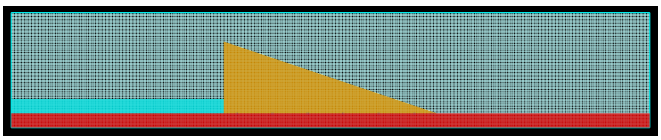

Figure 1. Mesh block anisotropy models

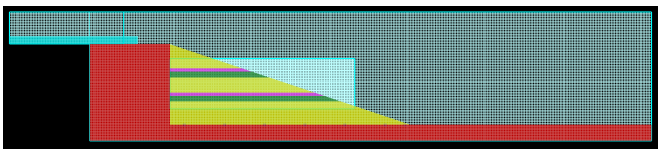

2.3 Border and Initial conditions

X_{min} condition is the inflow of the water normal to block surface; X_{max} consider the water outflow; Y_{min}, Y_{max} are assigned "wall" type with minimum roughness. The channel base Z_{min}, has its own characteristics (rigid and non-deformable surface) with roughness 0.003m (smooth mortar) similarly as the laboratory facility. Geometric fluid region was defined at the beginning of the simulation (t=0).

Figure 3. Arrangement and thickness of each layer within anisotropic shoulder.

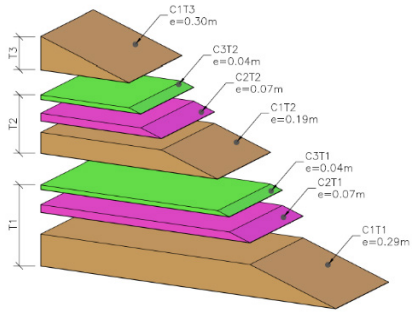

3 Physical calibration and numerical tests

The research included two sets of numerical models in order to make the calibration tasks and then the numerical heterogenous models. The first one simulated the through flow seepage in a homogeneous and isotropic shoulder and the second model an inhomogeneous shoulder formed by isotropic layers of different permeabilities.

Based on the model used for the calibration tests, the shell was modified by introducing 3 layers each formed by 3 layers as well of different permeabilities. The upper layer (C1) corresponded to a highly altered zone product of the compaction crushing. The intermediate layer (C2) considered such a lower altered zone. Finally, the lower layer (C3) corresponding to an unaltered zone.

Layer C1 was made up of material used in the calibration tests. C2 and C3 were assigned to customary permeability values (Table 1) for medium and fine sands (Barnes, 2010) and (Juárez, Eulalio; Rico, Alfonso, 2005)

Table 1. Granulometry and permeabilities of layers C2 and C3

Test	Layer	d_{50}(mm)	∅	K (m/s)
P1	C2	10	0.39	$2.0 \cdot 10^{-1}$
	C3	6	0.37	$1.0 \cdot 10^{-2}$
P2	C2	8	0.39	$2.0 \cdot 10^{-1}$
	C3	4	0.37	$1.0 \cdot 10^{-3}$

The physical model was developed in a 9.0m long 0.20m wide horizontal channel. The rockfill sample was 1,0m high with 3H:1V downstream slope (Figure 4). The numerical model was reduced to width of 0.10m to be able to decrease the mesh size and simulation durations. The physical model involved 3 zones of 3m long each. The first is to permit the approximation of the flow; the second is where the granular sample is located, and the third downstream, where the outflow occurs. In the channel base there are 7 points to measure pressure heads in the longitudinal direction X.

The granular material used in the physical calibration tests had a diameter d_{50}=12.6mm and a porosity ∅=0.41. The full characteristics of this material can be consulted at (Morán, 2013).

Figure 4. Physical model of homogeneous and isotropic rockfill.

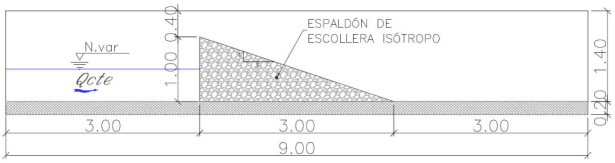

The characteristics of the numerical model considering the anisotropy were similar to those that have been raised in the calibration tests, with exception of the approach zone located at the crest of the sample to simulate an inflow by overtopping (Figure 5).

Figure 5. Numerical model considering anisotropy

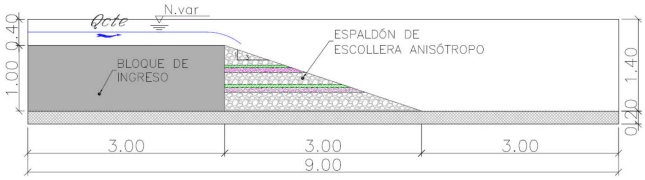

Tests were made for the same unit discharges used in the physical calibration: q_1=4.2ls^{-1}m^{-1}; q_2=13.5ls^{-1}m^{-1} and q_3=22.8ls^{-1}m^{-1}. In this campaign, two numerical models were carried out, each for two unit discharges, considering a variation in permeabilities of layer 3 showed in Table 1. Layer thicknesses may be observed in Figure 3. The measure points are coincident with the one used in the physical tests.

4 Results

4.1 Calibration

Figure 6 shows variation in time of pressures, inflows and outflows for test for a unit discharge of 22.8ls^{-1}m^{-1}. Results were obtained until flow was stabilized. Table 2 shows pressure heads at one of the measurement points and compared with laboratory tests. The errors

(%Err) are expressed as a percentage of physical model value taken as a reference.

Figure 7 shows pressure variation lines between numerical model and laboratory tests. With these results, parabolic relation between hydraulic gradient and average seepage velocity has been determined and resistance law checked according to the methodology proposed by Morán (2013). Thus, resistance law obtained from laboratory tests was the following:

$$i = 2.710 \cdot u + 65.350 \cdot u^2 \qquad (9)$$

Figure 6. Evolution over time of (a) pressure head, (b) inflow and outflow discharges; q_u=22.8ls^{-1}m^{-1}

(a)

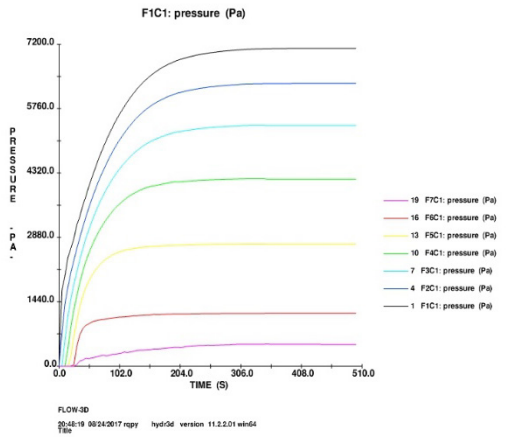

(b)

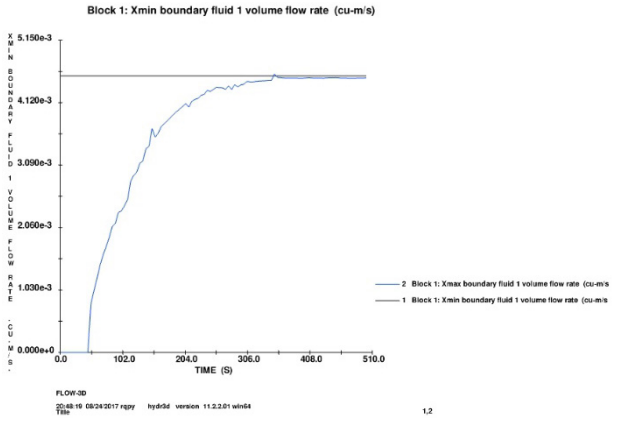

Table 2. Pressure head comparison (P) obtained in laboratory tests and Flow-3d code for qu_1=4.2ls^{-1}m^{-1}

Point	Pressure head (m)		
	Phys. model	Num. model	%Err
F1	0.331	0.287	13.041
F2	0.310	0.262	15.578
F3	0.289	0.233	19.355
F4	0.254	0.198	21.783
F5	0.207	0.155	24.925
F6	0.128	0.086	33.316
F7	0.058	0.017	70.181
F1	0.331	0.287	13.041

The mesh border condition allows to obtain inflow and outflow rates (Table 3) to determine the model convergence and volume continuity.

Table 3. Inflow and outflow within the domain

qu infllow (ls^{-1}m^{-1})	qu outflow (ls^{-1}m^{-1})	%Error
4.200	4.088	2.663
13.500	13.386	0.848
22.800	22.637	0.715

Figure 7. (a) Comparison of pressure heads between physical (subindex mf) and numerical models (subindex mn). (b) Map of pressure heads for q_u=22.8ls^{-1}m^{-1}

(a)

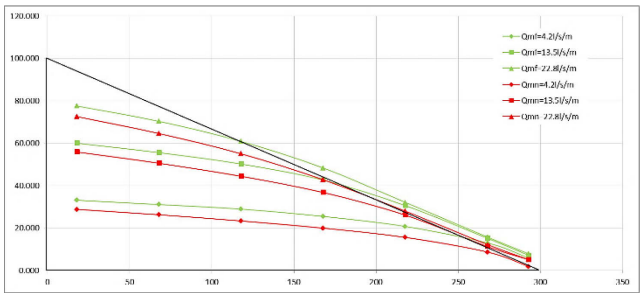

(b)

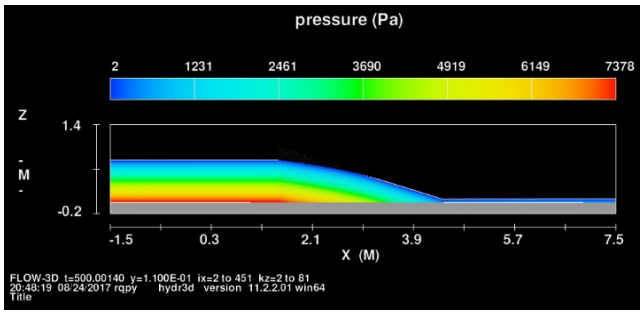

4.2 Heterogeneous models

The pattern of the saturation process within the heterogeneous rockfill is a key aspect to be able to interpret the numerical results exposed later on. Figure 8 shows the seepage evolution in a heterogeneous porous media formed by adjacent isotropic layers of different permeabilities for an overtopping unit discharge of qu=24.32ls^{-1}m^{-1}.

Test 2 (P2 in Table 4 and 5) includes a change in the material properties of the altered layer (C3) with a lower permeability compared to Test 1 (P1 in Table 4 and 5).

Figure 9 shows the variation in time of pressures, inflows and outflows for tests with unit flow rate of 22.8ls^{-1}m^{-1}.

Figure 8. Saturation process of a heterogeneous rockfill made of isotropic layers of different permeabilities, qu=24.32ls^{-1}m^{-1}. (a) Time=7s; (b) Time=17s; (c) Time=36s; (d) Time=70s.

(a)

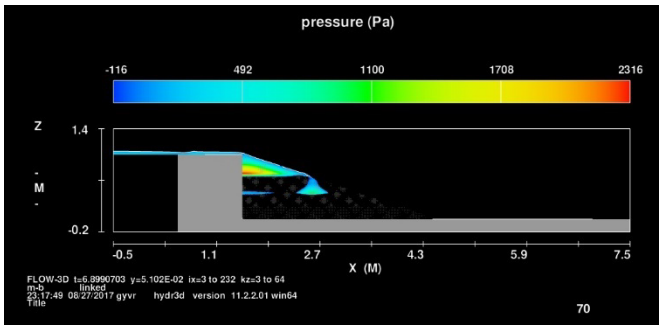

(b)

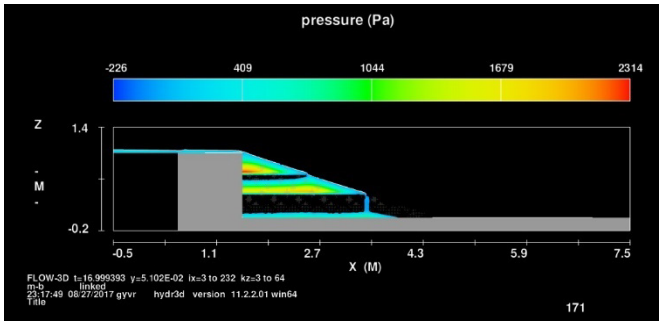

(c)

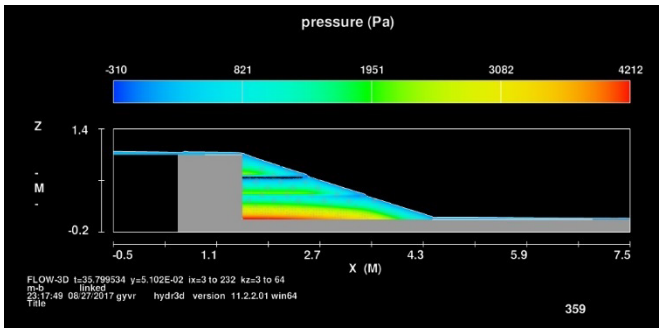

(d)

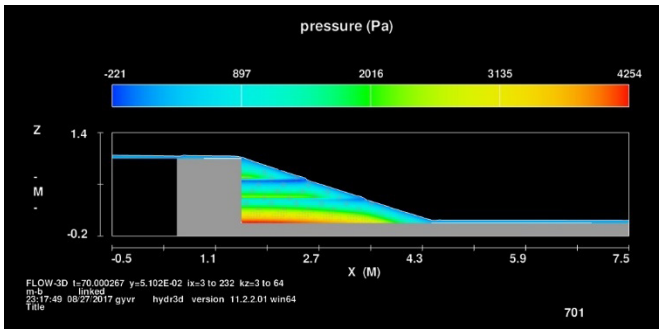

Table 4 and 5 show pressure heads of the models for each unit discharge. Figure 10 shows the profile of pressure heads and flow depths along the cross section.

Figure 9. Evolution over time, q_u=22.8ls^{-1}m^{-1} (a) pressure head, (b) inflow and outflow discharges.

(a)

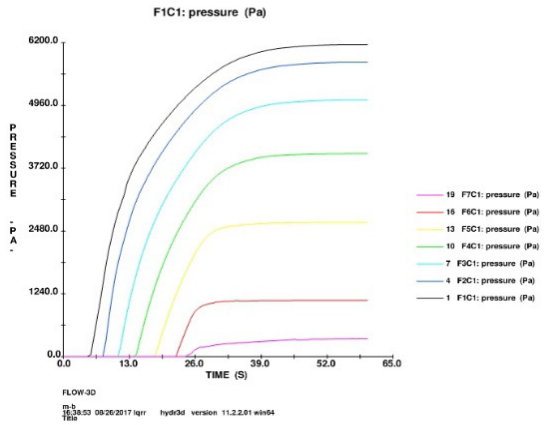

(b)

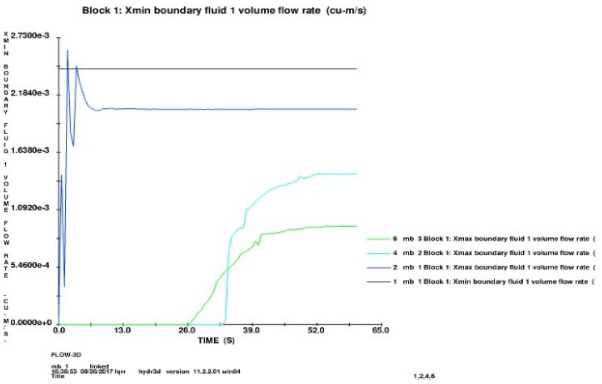

Table 4. Pressure heads for qu_1=14.55ls^{-1}m^{-1}

Point	Pressure Heads P(cm)				
	Phys. Mod	P1	%Err P1	P2	%Err P2
F1	59.93	48.92	39.36	18.36	34.32
F2	55.48	45.68	38.41	17.66	30.77
F3	50.10	39.91	36.11	20.33	27.92
F4	42.50	32.94	32.27	22.48	24.06
F5	30.45	24.23	24.60	20.42	19.22
F6	16.10	10.79	10.85	33.00	32.60
F7	7.00	2.80	2.88	60.04	58.93

Table 5. Pressure heads for qu_1=24.32ls^{-1}m^{-1}

Point	Pressure Heads P(cm)				
	Phys. Mod	P1	%Err P1	P2	%Err P2
F1	77.48	62.80	43.30	18.94	44.11
F2	70.23	59.23	42.29	15.66	39.79
F3	60.75	51.65	39.81	14.98	34.46
F4	48.20	40.86	35.76	15.23	25.80
F5	31.95	27.03	26.67	15.38	16.52
F6	17.00	11.33	11.38	33.36	33.04
F7	7.70	3.60	3.73	53.27	51.55

Figure 10. (a) profile of pressure heads (b) flow depths variation

(a)

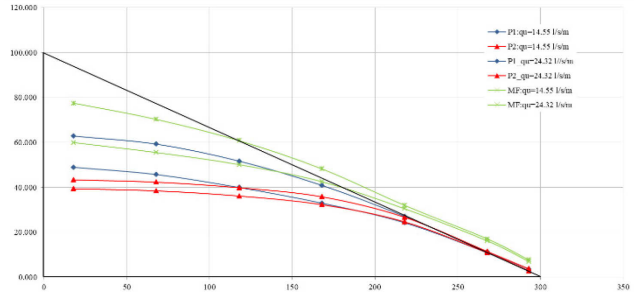

(b)

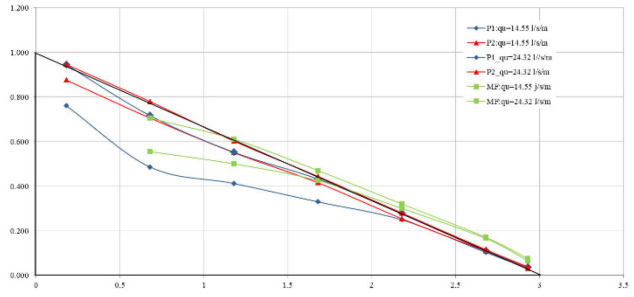

5 Discussion

5.1 Calibration

The results show that simulation stabilizes at a certain time. Figure 6 shows that after approximately 380 seconds the pressure heads remain constant. Figure 6-b and Table 3 show inflow discharge remains constant while outflow discharge increases as the shoulder becomes saturated. the relative error in relation to inflow is 2.663% for $4.2ls^{-1}m^{-1}$; 0.848% for $13.5ls^{-1}m^{-1}$ and 0.715% for $22.8ls^{-1}m^{-1}$ at the end of simulation time. The development of a numerical model implies certain simplifications in relation to real condition that reduce the problem complexity, which can lead to errors that have to be evaluated. In border conditions Y_{min} and Y_{max} have been defined as "wall" type. Although the code assigns default characteristics such as roughness and considers the mesh faces to behave like a wall, it can differ significantly in relation to a laboratory test whose roughness coefficient can have values of tenths of millimeter up to several millimeters depending on the finished quality. In this case, a solid object with a rigid and non-deformable surface and an absolute roughness of 0.003 has been arranged, which corresponds to a finishing coat with plastered mortar. As Table 2 shows, the differences on pressure heads between numerical models and laboratory tests oscillated between absolute values of 2.05cm to 8.85cm and remain of the same order of magnitude in every case. This error, expressed as a percentage of experimental value, ranged between 13.04% in F1 located at the upstream measure point and 70.18% in F7 near the downstream toe. This pressure difference decreased as seepage flow rate increased. The tests with unit flow discharge of 13.5 and $22.8ls^{-1}m^{-1}$ show a lower error percentage in the two downstream measuring points (F6 and F7).

5.2 Heterogeneous models

Before discussing numerical results, saturation process of the heterogeneous rockfill shell formed by different layers is described. As it can be seen in Figure 8, the water inflows by the crest and leaks through the upper layer in a sub vertical direction until reaching the first altered layer. In this sector, the water begins to accumulate due to a lower material permeability that partially prevents water to flow towards the lower layer. One fraction of the flow advances downstream in a nearly horizontal direction as the other leaks vertically towards the next layers underneath. The process is repeated until reaching the impervious base where the water accumulates filling the empty voids as flows towards the toe of the slope. Obviously, as the altered layer lowers its permeability, the velocity of saturation of the upper layers increases. Figure 8-a shows that the upper zone has been saturated almost completely until reaching the outer face of the slope where a vertical drop occurs to the next layer of greater permeability. The same happens with the next layer shaping "steps" (Figure 8-b). The model agrees with the hypothesis proposed by Toledo (1997), who stated that the upper area of the rockfill shell can be completely saturated before the water has reached the bottom if the permeability is low enough. That could lead to mass sliding and dragging processes near the crest of the dam. This could be serious, since the loss of the material of the shell in that area may leave the core or impervious face without support and vulnerable to a potential failure. Results of Test 2 with a flow rate of $24.32ls^{-1}m^{-1}$, shows the saturation of the shell is almost complete without any free voids between layers (Figure 8-d).

The results of the heterogeneous model show that flow presents liquid vein ruptures in several points of layer. This "drip" effect that occurs during vertical leakage

through altered layers makes it difficult to measure pressure heads and flow depths as can be seen in Figure 10 compared to Figure 8. The flow depth at the toe is higher while altered layer permeability decreases. This can be seen in Figure 8-d where the saturation is almost complete, and the skimming flow appears over the slope with low unit discharges which does not happen with homogeneous and isotropic shells.

6 Conclusions

The compaction effect in rockfill dams during construction varies the granulometry of the surface layers of each lift. Such effect causes variations in the permeability in the vertical direction, which significantly influence the saturation process of an eventual overtopping. In the present work, the flow through a heterogeneous rockfill shell formed by isotropic layers of different permeabilities has been modeled numerically using Flow-3D code. The saturation process of the heterogeneous shell may cause the partial or complete saturation of the upper layers as a function of the permeability of altered layers and the magnitude of overtopping flow.

In a real dam, this could be serious, since the loss of the material of the shell in that area may leave the core or impervious face without support and vulnerable to a potential failure

Numerical models present limits of accuracy in their results due to some simplifications that they adopt to reduce the complexity of some processes. In order to improve the accuracy of the results it is advisable to deepen on the characterization of the different parameters that influence the real processes.

Acknowledgment

To the Ministry of Science and Innovation for the means provided for this research based on the project "Rotura del elemento impermeable de presas de materiales sueltos en situación de sobrevertido y análisis de protecciones combinando modelación física e inteligencia artificial", with code BIA2010-21350-C03-03 concerning National Plan I+D+i 2008-2011. The authors also gratefully acknowledge the company "Proyectos y Simulaciones, SL" for their collaboration in providing technical support for the use of Flow-3D code.

References

Barnes, G., 2010. *Soil Mechanics: Principles and Practice.* s.l.:s.n.

Cruz, P. T., Materon, B. & Freita, M., 2010. *Concrete Face Rockfill Dams.* s.l.:CRC Press.

Flow Science, 2015. *Flow-3D version 11.1. User manual.* s.l.:s.n.

Juárez, Eulalio; Rico, Alfonso, 2005. *Mecánica de Suelos Tomo I. Fundamentos de la Mecánica de Suelos.* s.l.:Limusa.

Morán, R., 2013. *Mejora de la seguridad de las presas de escollera frente a percolación accidental mediante protecciones tipo repié.* Madrid: Tesis doctoral: Universidad Politécnica de Madrid.

Morán, R., 2014. Review of embankment dam protections and a design methodology for downstream rockfill toes. *1st International Seminar on Dam Protections Against Overtopping and Accidental Leakage.*

Morán, R. & Toledo, M. Á., 2011. Research into a protection of rockfill dams from overtopping using rockfill downstream toes. *Canadian Journal of Civil Engineering,* p. 13.

Toledo, M. Á., 1997. *Presas de escollera sometidas a sobrevertido. Estudio del movimiento del agua a través de la escollera y de la estabilidad frente al deslizamiento en masa.* Madrid : Tesis doctoral.

Toledo, M. Á., Morán, R. & H., C., 2012. Modelación del movimiento del agua en medios porosos no lineales mediante un esquema de diferencias finitas. Aplicación al sobrevertido en presas de escollera. *Revista Internacional de Métodos Numéricos para Cálculo y Diseño en Ingeniería,* p. 12.